Characterization of GaAs Nanoparticles by Laser Ablation Dispersed in Acetone

Atyaf S. AL Rawas
Dept. of Basic Science, College of Dentistry, Mosul University, Iraq.
Muna Y. Slewa
Dept. of Physics, College of Education, Al-Hamdaniya University, Iraq.
Fatin M. Hamam
Dept. of Basic Science, College of Dentistry, Mosul University, Iraq.
Najeeb M. Nooh
Dep.of Physics, College of Education, Al-Hamdaniya University, Iraq.

Abstract

This paper demonstrates the optical band gap and optical constants of Gallium arsenide GaAs nanoparticles through laser ablation into liquids LAL technique from a solid GaAs target immersed in acetone by irradiating using Nd Pulsed: YAG laser works at 64 = 1064 nm (HUAFEI type), 7ns pulse width and 10Hz frequency. The laser flow used for ablation was fixed at 1.32 J/ cm2 and the ablation time was 5min. The band gap energy is calculated by generating GaAs particles immersed in the acetone via the touch method to be 3.8EV, which is greater than the band gap energy of bulk GaAs. The optical constants of the GaAs submerged in acetone were made in the UV/ Visible region (300-1200nm). It has been found that transmission spectra are increasing by increasing wavelength, while optical absorption coefficients, extinction coefficient and refractive coefficient decrease. The stability of acetone was studied using the Z-Scan Brookhaven Instruments Corporation Holtsville, NY 11742 US to measure the potential of the Z for GaAs particles drilled in acetone. The Z-potential was calculated using an approximation such as the Smoluchowski formula.

Keywords: laser ablation, GaAs nanoparticles, band-gap energy, optical constants, Zeta potential.

????? ١٩

???

.????

???

.???

المستخلص

يوضح هذا البحث فجوة النطاق البصري والثوابت البصرية لجزيئات زرنيخيد الغاليوم من خلال تقنية القشط بالليزر في السوائل والهدف هو زرنيخيد الغاليوم الصلب المغمور في الأسيتون عن طريق التشعيع باستخدام ليزرالنيوديميوم – ياك النبضي الذي طوله الموجي ١٠٦٤ نانومتر، وعرض النبضة ٧نانوثانية وعند تردد ١٠هيرتز. تدفق الليزر المستخدم في القشط كان ١,٣٢جول/سنتيمتر مربع وكان زمن التشعيع المستخدم في القشط ٥ دقيقة على الأقل. تم حساب طاقة فجوة النطاق عن طريق توليد جزيئات زرنيخيد الغاليوم المغمورة في الأسيتون عن طريق اللمس وسجلت ٣,٨ الكتروفولت لتكون أكبر من طاقة فجوة النطاق لزرنيخيد الغاليوم. تم قياس الثوابت البصرية لزرنيخيد الغاليوم المغمور في الأسيتون في المنطقة المرئية للاشعة فوق البنفسجية. وجد أن أطياف الإرسال تتزايد بزيادة الطول الموجي ، بينما تنخفض معاملات الامتصاص البصري ومعامل الانقراض ومعامل الانكسار. تمت دراسة ثبات الأسيتون باستخدام جهاز المسح Z، لقياس إمكانات جسيمات زرنيخيد الغاليوم المحفورة في الأسيتون. تم حساب الإمكانات باستخدام صيغة التقريب Smoluchowski.

الكلمات المفتاحية: .

Introduction

Semiconductor quantum points and nanoparticles (NPs) have attracted wide interest through past decennium especially because of their optoelectronic implementations. The size-dependent band-gap energy and constructs of these NPs make it possible to styling a composite material with tunable optical and electrical characteristics. Different semiconductors, like GaAs have obtained a large significant due to its broad area from applicability in apparatus physics [1][2].

The most interesting dot regarding the semiconductor NPs is displayed for novel optical, structural and electrical properties so several of selfsame of their bulk counterparts. Especially, when the bulk of the NCs is near to or least than the exciton Bohr radius within the congruent bulk material, they are named quantum points and display very particular natural and alchemical effects. Between the different methods for preparation of GaAs NCs, laser ablation has been used via different interrogators to synthesize this semiconductor component, either in the gas or in liquid mediums [3][4].

Solid state lasers need less maintenance, but they usually work at longer wavelengths that are not absorbed as efficiently. The most commonly used solid state laser material is Nd: YAG, which emits a wavelength of 1064 nm. To improve absorption, nonlinear crystals are used to reduce the wavelength of the laser by a second or third coordinated configuration [4][5].

PLAL is a versatile and versatile method of use for the installation of nanoparticles. Particles produced are clear, excellent and suitable for further operation and can be easily incorporated into polymer matrices [6]. The process can be run continuously, and has recently been showing average production of several grams per hour. The interaction of the laser pulses was studied in a liquid steel medium to modify the iron to create a surface layer of metastatic oxide phases [7]. PLAL was described for the generation of nanoparticles in the early 1990s. The first report was to monitor the diamond particles after irradiation of a pulsed laser ruby for a sample of graphite in gasoline [8].

PLAL tests are usually performed under ambient conditions (room temperature, atmospheric pressure) with a sample immersed in a constant liquid or which is transparent in the laser wavelength used [9]. Zeta-potential ZP is a surface charging indicator that improves when any material is placed in a liquid. It is a precise indicator of the amount of electrical repellent interaction between particles. ZP is usually applied to predict and control scatter stability. The liquid liquid interface property may also affect, inter alia, adhesion and buoyancy and in more concentrated systems, in a theological manner. Therefore, reliable ZP decisions are a practical concern for many manufacturers, including ceramic preparation, processing and application [10][11].

Interest in the synthesis, description and application of quantum point materials for semiconductors has increased significantly since these studies lead to space dares through solid atoms. This growing interest reflects both the strong dependence on the size of the optical and electronic properties of these materials, and the fact that materials make it relatively easy thanks to good particle size control [12].

In this paper optical property deduced from optical transmittance, optical absorption coefficients, extinction coefficient and the refractive coefficient at room temperature were studied. The absorption index was applied to obtain an optical band gap for GaAs dispersed in acetone and acetone stability was studied.

Material and Methods

Diagram of laser ablation in a liquid system for nanoparticles appears in Fig.1. The GaAs nanoparticles pressed pellet having diameter of $1cm^2$ Located at the bottom of a glass container, filled with acetone so the solution is 0.5 cm on GaAs nanoparticles. GaAs nanoparticles is ablated using Nd: YAG laser worked at λ=1064nm (type HUAFEI), Focused by a Plano convex lens length of 8 cm on the surface GaAs nanoparticles. The laser flow used for ablation was fixed at 1.32 J / cm2 and the ablation time was 5min.The GaAs nanoparticles are an optical good to explain the quantitative influence inside chemistry, since their transition energies can be demonstrated as a “particle in a box,” where the delocalized electron is a particle and nanoparticle is a square. The band - gap energy of producing GaAs nanoparticles was calculated which greater than the band gap energy of bulk GaAs. Absorption spectra for colloid soil were measured using UV-Visible. The stability of the acetone was studied using a Z-scan Brookhaven Instruments Corporation Holtsville, NY 11742 US for measurement zeta-potential of the GaAs nanoparticles immersed in Acetone Zeta-potential was calculated by using an approximation such as the Smoluchowski formula.

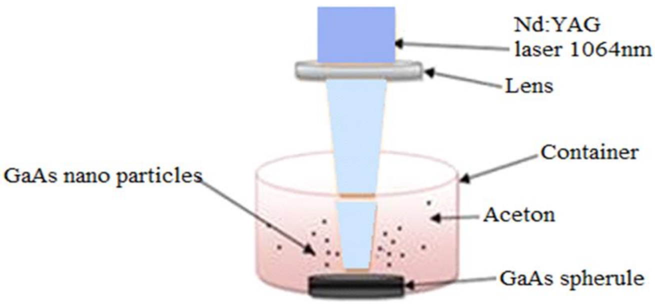

Fig. 1: Schematic diagram of laser ablation in liquid system for nanoparticles which are prepared with 1.32 J/cm2 laser fluence

Results and Discussion

Optical properties of GaAs nanoparticles immersed in acetone have been investigated by UV–VIS spectrometer at room temperature, the transmission spectra of GaAs nanoparticles immersed in acetone as the function for the wavelength appears in Fig.2. These nanoparticles showed good transparency (between 75% and 95%) in the visible and infrared regions (600-1100) nm. The sharp decrease in the direction of the ultraviolet (less than 350 nm) area is due to the primary absorption of light caused by the excitation of electrons from the range of the valence range. Optical absorption index α of samples are estimated from their transmittance spectrum use following relation [13].

$$\alpha = 1/t\ [\ln (1/T)]$$

Where t is the thickness and transfer of T. The energy gap was estimated for example from GaAs nanoparticles using a touch relationship see Fig.3 [14]. The results obtained are given in Fig.4 indicating the difference in the absorption coefficient as a function of wavelength. It has seen the absorption coefficient decrease when the wavelength increases.

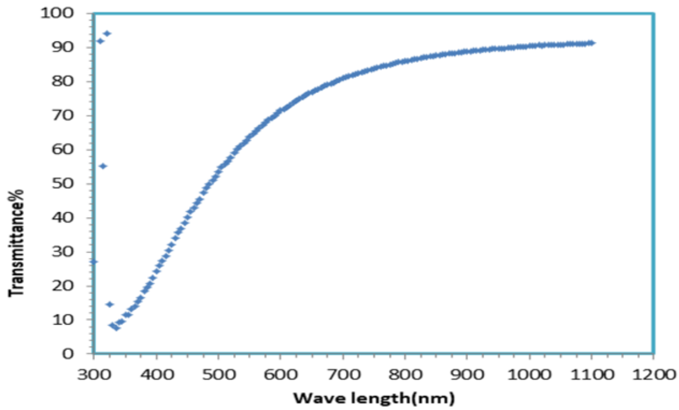

Fig. 2: Transmittance spectra of GaAs nanoparticles immersed in Acetone as a function of wave length

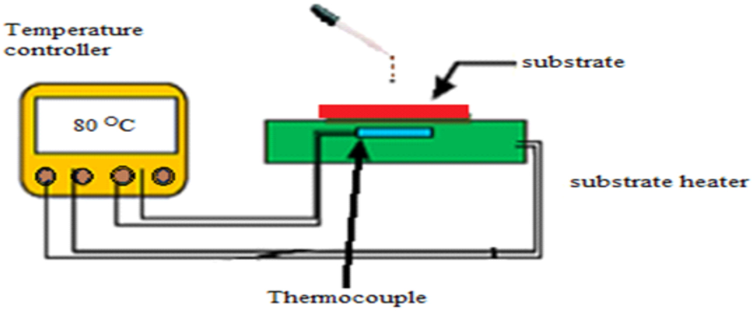

Fig. 3 Schematic diagram drop molding method experimental set up

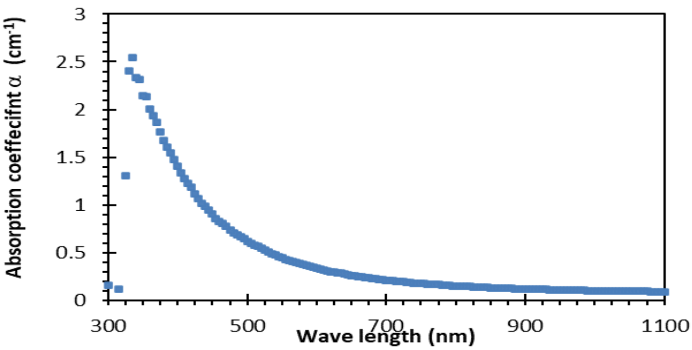

Fig. 4: Absorption coefficient versus wavelength for GaAs nanoparticles immersed in Acetone

Visual absorption was analyzed using the following equation [15][16].

$$\alpha h\nu = A\,(h\nu -)^{1/2}$$

Where A is constant, hν is the photon force. The band gap of Figure 5, which shows that a plot of $\alpha h\nu$ ^{2} vs. hν of the GaAs submerged in acetone, is linear in the wide range of photon energies that indicate a direct type of transitions. The intersections of these plots reflect the energy axis of the energy bar gaps; give the junction of the rectangle with the high voltage axis gap in the range (E_g) 3.8 volts due to the retention of the quantum.

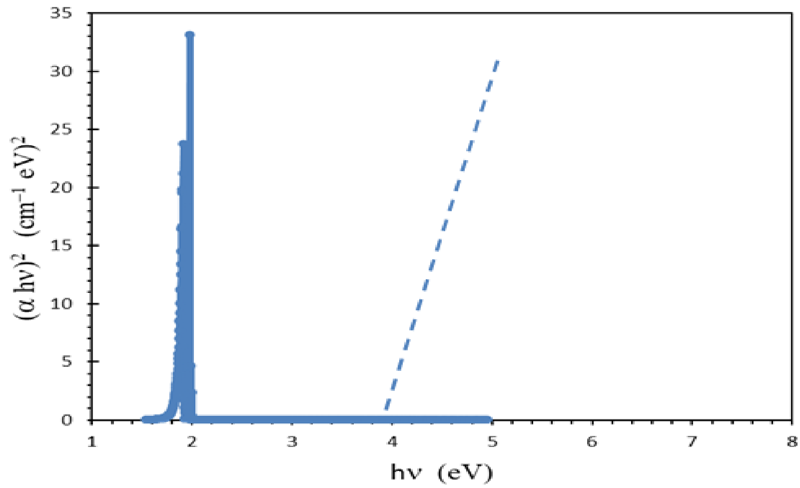

Fig. 5: Variation of (α h ν)^2 vs. h ν of the GaAs nanoparticles immersed in Acetone

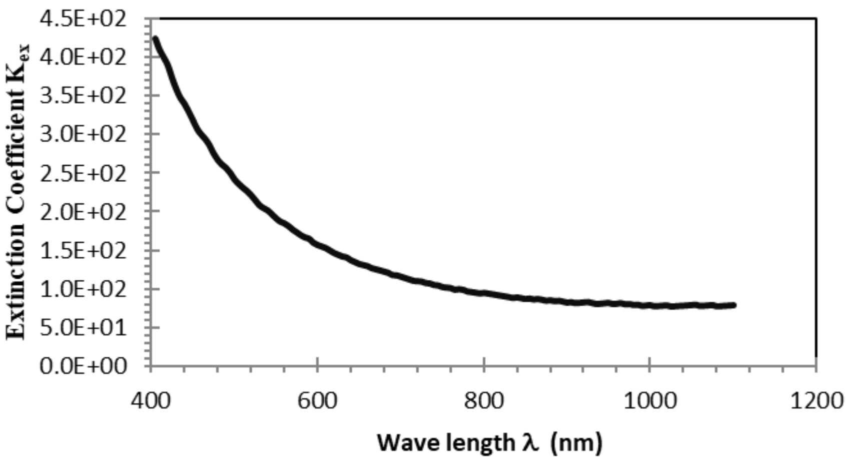

Fig. 6: Extinction coefficient k_{ex} for GaAs nanoparticles immersed in Acetone as a function of wavelength

To complete the calculation of optical constants, the k_{ex} extinction index is evaluated from the values of the α and λ wavelength using the formula:

$$k_{ex} = \alpha\lambda / 4\pi \text{ [17].}$$

Figure (6) shows Dependence on the K_{ex} extinction coefficient versus wavelength of GaAs nanoparticles immersed in acetone. This absorption of the electromagnetic wave factor is characterized by the propagation of the wave across the material. The effects of dispersion and lighting are also taken into consideration.

The refractive index (n) of GaAs is determined in different combinations of GaAs nanoparticle. The GaAs reflects the peaks in transitions between the bands. The value of the spectral refractive index curves (n) determines the next use of the relationship [18][19].

$$R = \frac{(n-1)^2 + k_{ex}^2}{(n+1)^2 + k_{ex}^2}$$

Where R is the reflectance. The dependence of the refractive index (n) of GaAs nanoparticles immersed in Acetone on the wavelength λ is shown in the Fig. 7. Difference in refractive index (n) with the wavelength in the range 850–1100 NM, refractive index has been found to decrease with increase the wavelength. The Zeta-potential of the samples for acetone was prepared measured to be −0.69 mV.

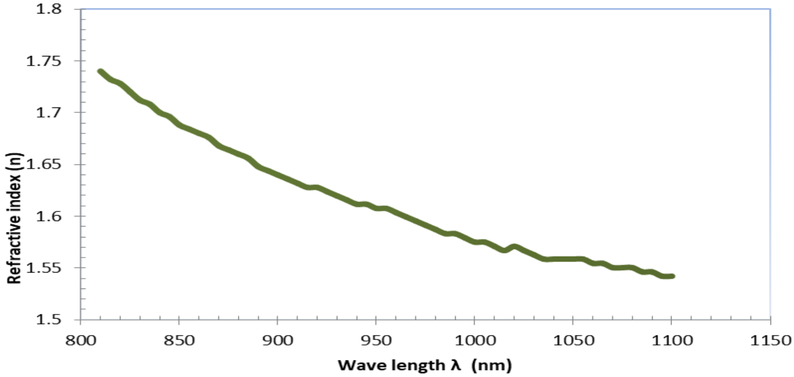

Fig. 7: Refractive index (n) for GaAs nanoparticles immersed in Acetone as a function of wavelength

The stability of the acetone was studied using a Z-scan to measure the zeta-potential of the GaAs nanoparticles immersed in Acetone. The figures (8, 9, 10, 11) A typical ELS spectrum was obtained with a 1064nm wave length. The central peak is called the reference peak without an applied electric field. Sample peak frequency is -0.14 Hz that corresponds to electrical mobility equal -0.01 volts / m and Zeta - potential -0.69 mV assuming the Smolchovsky boundary, then peak of GaAs nanoparticles immersed in Acetone is wider than the reference peak indicating the range of zeta potential within the sample rather than the single value.

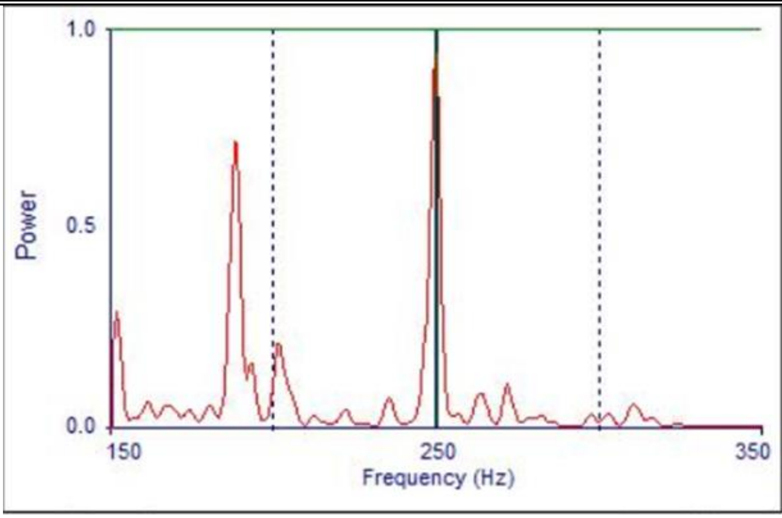

Fig. 8: The power spectrum as a function of frequency (249.86 Hz) peak

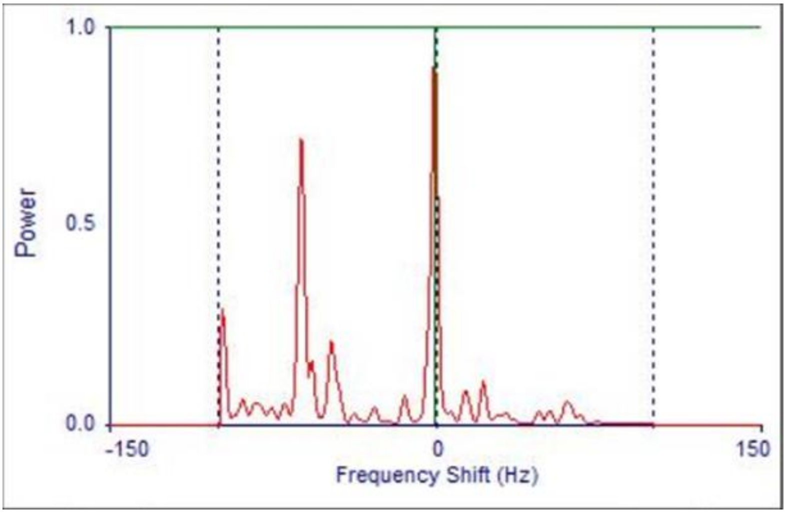

Fig. 9: The power spectrum as a function of the frequency ship (-0.14) Hz

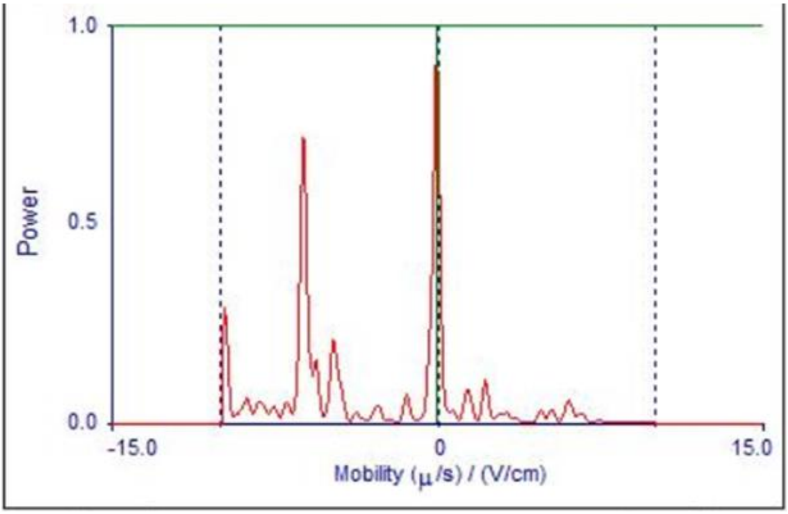

Fig. 10: The power spectrum as a function of the Mobility (-0.01) v/cm peak

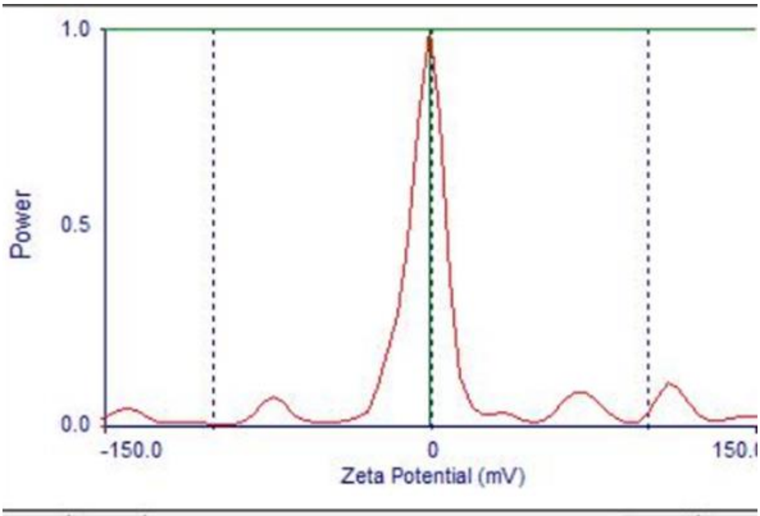

Fig. 11: The Power spectrum as a function of Zeta potential (-0.69mv) peak

Conclusion

Optical absorption measurements for GaAs nanoparticles immersed in Acetone Conducted in the UV / visible area (300-1200 nm). The transmission spectra were found to increase by wavelength, while optical absorption, extinction and refractive index decreased. The visual transport type responsible for optical absorption was indirect. On the basis of the visible investigations of molecules, the following results were obtained according to the Tauc capacitor gap energy, and the band gap energy in the nanoparticles generating 3.8eV is greater than the band gap energy of bulk GaAs which is about 1.42eV [20][21].

The power spectrum obtained for 1064nm wavelength is reference peak with frequency shifted -0.14Hz that is compatible with electric mobility of -0.01v/m and zeta-potential of -0.69 mV. The peak of the sample is wider than the reference peak indicating the range of zeta-potential in the sample rather than the single value. When nanoparticles move vertically on a laser beam, the scattered light frequency is shifted. This shifted frequency contains the facts on the electrophoretic mobility. Since frequency is inherently positive, it is necessary to add a reference beam to separate positive and negative transformations. Frequency shifts greater than the local oscillator frequency grows from positively charged particles. Frequency Transitions less than the frequency of the local oscillator arise from the negatively charged particles of the local oscillator frequency in Zeta-potential is 250 Hz. Frequency shifts are generally less than 100 Hz [22].

Acknowledgments

The research is supported by Dr. Odai N. Salman University of Technology/ Department of Applied Science .

References

[1] Nayak J., Sahu S.N., and Nozaki S., GaAs Nanocrystals: structure and optical properties, Appl. Surf. Sci. 252 (2006), pp. 2867–2874.

[2] Rawas, A. S. A., Slewa, M. Y., Bader, B. A., & Fadhil, N. (2020). Physical characterization of nickel doped nanostructured TiO2 thin films. Journal of Green Engineering, 10, 7141-7153. Ganeev RA, Baba M, Ryasnyansky AI, Suzuki M, Kuroda H. Laser ablation of GaAs in liquids: structural, optical, and nonlinear optical characteristics of colloidal solutions. Applied Physics B. 2005 Apr 1;80(4-5):595-601.

[3] Spühler GJ, Paschotta R, Fluck R, Braun B, Moser M, Zhang G, Gini E, Keller U. Experimentally confirmed design guidelines for passively Q-switched microchip lasers using semiconductor saturable absorbers. J. Opt. Soc. Am. B. 2001 Jun 1;18(6):886.

[4] Hadi, E. H., Salih, F. M. H., Slewa, M. Y., Bader, B. A., & Habubi, N. F. (2020). Fabrication and Characterization of Vanadium Doped Nanostructured Cdo Thin Films to Improve the Energy Band Gap. Journal of Green Engineering, 10, 7195-7207.

[5] Zeng H, Du XW, Singh SC, Kulinich SA, Yang S, He J, Cai W. Nanomaterials via laser ablation/irradiation in liquid: a review. Advanced Functional Materials. 2012 Apr 10;22(7):1333-53.

[6] Bain CD, Troughton EB, Tao YT, Evall J, Whitesides GM, Nuzzo RG. Formation of monolayer films by the spontaneous assembly of organic thiols from solution onto gold. Journal of the American Chemical Society. 1989 Jan;111(1):321-35.

[7] Ahmed, N. Y., Bader, B. A., Slewa, M. Y., Habubi, N. F., & Chiad, S. S. (2020). Effect of Boron on Structural, Optical Characterization of Nanostructured Fe2O3 thin Films.

NeuroQuantology, 18(6), 55. Camarda P. Growth and photoluminescence dynamics of zno nanoparticles produced by pulsed laser ablation in liquid.2017.
[8] Bhattacharjee S. DLS and zeta potential–What they are and what they are not? Journal of Controlled Release. 2016 Aug 10; 235:337-51.
[9] Weiner BB, Tscharnuter WW, Fairhurst D. Zeta potential: a new approach. InCanadian Mineral Analysts Meeting 1993 Sep 8 (Vol. 12).
[10] Guozhong C. Nanostructures and nanomaterials: synthesis, properties and applications. World scientific; 2004 Apr 8.
[11] Swanepoel R J. Phys. E: Sci.Instrum. 16 (1983) 1214.
[12] Ganeev R.A., Baba M., Ryasnyanskiy A.I., Suzuki M., and Kuroda H., Laser ablation of GaAs in liquids: Structural, optical, and nonlinear optical characteristics of colloidal solutions, Appl. Phys. B 80 (2005), pp. 595–601.
[13] Mott N.F., Gurney R.W., Electronic Processes in Ionic Crystals, Oxford Univ. Press, London, 1940.
[14] Robertson J., Phil. Mag. B 63 (1994) 307.
[15] Essahlaoui A., Roemer A., Boudrioua A., Million E., Loulergue J. C., Opt. Mater. 24(3) (2003) 465-470. 20.
[16] Ziang X, Shifeng L, Laixiang Q, Shuping P, Wei W, Yu Y, Li Y, Zhijian C, Shufeng W, Honglin D, Minghui Y. Refractive index and extinction coefficient of CH 3 NH 3 PbI 3 studied by spectroscopic ellipsometry. Optical Materials Express. 2015 Jan 1;5(1):29-43.
[17] Durgam Komaraiah ER, Vijayakumar Y, Sivakumar J, Reddy MR, Sayanna R. Optical, Structural and Morphological Properties of Photocatalytic ZnO Thin Films Deposited by Pray Pyrolysis Technique (2016).
[18] Srivastava A, Srivastava R, Wang J, Kono J. Laser-induced above-band-gap transparency in GaAs. Physical review letters. 2004 Oct 4;93(15):157401.

[19] Saunders WA, Sercel PC, Atwater HA, Vahala KJ, Flagan RC. Vapor phase synthesis of crystalline nanometer-scale GaAs clusters. Applied physics letters. 1992 Feb 24;60(8):950-2.

[20] Kumar P, Bohidar HB. Physical and fluorescent characteristics of non-functionalized carbon nanoparticles from candle soot. Journal of Nanoparticle Research. 2012 Jul 1;14(7):948.

[21] Brans T. Optical trapping electrophoresis for label-free biodetection (Doctoral dissertation, Ghent University) (2015).

[22] Foster EJ, Moon RJ, Agarwal UP, Bortner MJ, Bras J, Camarero-Espinosa S, Chan KJ, Clift MJ, Cranston ED, Eichhorn SJ, Fox DM. Current characterization methods for cellulose nanomaterials. Chemical Society Reviews. 2018;47(8):2609-79.